Iraqi Journal of Science, 2020, Vol. 61, No. 6, pp: 1383-1391
DOI: 10.24996/ijs.2020.61.6.16

ISSN: 0067-2904

Paleostress Analysis of Chia Gara Structure in Dohuk Area, Northern Iraq

Atheer E. K. AL- Hachem
Department of Geology, College of Science, University of Baghdad, Baghdad, Iraq

Received: 27/10/2019 Accepted: 21/1/2020

Abstract

The use of Right dihedral method, Lisle graph, and Mohr diagram allows the analysis of the paleostress. Fault slip data were measured for eighteen data of two stations located within Chia Gara structure in Dohuk area in the High Folded Zone, Northern Iraq. Depending on Mohr diagram, Bott equation, and vertical thickness, the magnitudes of the paleostress at the time of the tectonic activity were determined. Firstly, Georient Software was used to estimate the orientation of the paleostresses (σ1, σ2 and σ3). Secondly, using the rupture –friction law, taking into account the depth of the overburden, the vertical stress (σv) was calculated to determine the magnitude of the paleostresses in the study area. The values in station one (hinge area, eight data) were σ1=7100, σ2=4121.5, and σ3=1143 bars, whereas the values in station two (the north limb of structure, ten data) were σ1=3740, σ2=1585, and σ3=570 bars. The high magnitudes of the principal stress axes may refer to the active tectonic events which led to the deformation of the area during the Mesozoic Era and the Tertiary period. The study area shows the existence of two types of the faults, the first type is the reactivated faults, the poles of which lie between the sliding line and Mohr envelope. The second type is the inactive faults, with poles lying on the great circle of Mohr diagram.

Keywords: Paleostress, Mohr diagram, Right dihedral method, High Folded Zone, Iraq.

تحليل الاجهاد القديم لتركيب جياكارا في منطقة دهوك شمال العراق

اثير عيدان خليل الحاجم
قسم علم الارض، كلية العلوم، جامعة بغداد، بغداد، العراق

الخلاصة

استخدمت طرق التعامد الثنائي, مخطط لايل ومخطط موهر لتحديد الاجهاد القديم لثمانية عشر قراءة للصدوع في محطتين, حددت ضمن تركيب جياكارا في منطقة دهوك في نطاق الطيات العالية شمال العراق. حددت قيم الاجهادات القديمة الرئيسة اعتمادا على طريقة موهر , معادلة بوت و السمك العمودي. اولا, استخدم برنامج جيواورينت لتحديد اتجاه الاجهادات القديمة (σ1 و σ2 و σ3) .

ثانيا,حددت قيم الاجهادات القديمة في المحطة الاولى في منطقة مفصل التركيب بالاعتماد على قانون الاحتكاك, معدل السمك والاجهاد العمودي والتي كانت قيمة الاجهاد الرئيسي الاعظم (σ 1) هي (7100) بار, كانت قيمة الاجهاد الرئيسي المتوسط (σ2) (4121.5) بار وكانت قيمة الاجهاد الرئيسي الاصغر (σ3) (1143) بار. اما في المحطة الثانية التي تقع في الجناح الشمالي للتركيب, كانت قيمة الاجهاد الرئيسي الاعظم (σ 1) هي (3740) بار, كانت قيمة الاجهاد الرئيسي المتوسط (σ2) (1585) بار وكانت قيمة

Email: atheergeo1980@scbaghdad.edu.iq

الاجهاد الرئيسي الاصغر (σ3) (570) بار. اوضحت الدراسة ان القيم العالية لمحاور الاجهادات الرئيسة ربما تعود الى الاحداث التكتونية التي حدثت خلال حقبة الحياة المتوسطة و فترة العصر الثلاثي. بينت الدراسة تواجد نوعين من الصدوع , النوع الاول , صدوع اعادة التنشيط التي, تقع اقطابها بين خط الانزلاق و غلاف موهر. اما النوع الثاني , الصدوع غير النشطة التي تقع اقطابها على الدائرة الكبيرة في مخطط موهر.

Introduction

Chia Gara Structure lies in Dohuk area of Northern Iraq. It runs approximately along the E-W direction forming a doubly plunging anticline located within the High Folded Zone of Iraq and extending parallel to the Taurus Belt in the south part of Turkey. The length of the structure is about 80 Km with a width of about 12 Km. It is located between latitudes (36° 56′ - 37° 03′ North) and longitudes (43° 02′ - 43° 56′ East) (Figure-1). There are several structural studies which were carried out on the High Folded Zone and Foothill Zone of Iraq and dealt with the orientation and magnitude of the paleostresses [1-6]. Generally, the state of paleostress in the rocks is anisotropic and is defined by stress ellipsoid axes, which characterizes the magnitudes of the principal stresses [7,8]. Most researches concerning fault slip data aimed to determine the principal stresses direction.

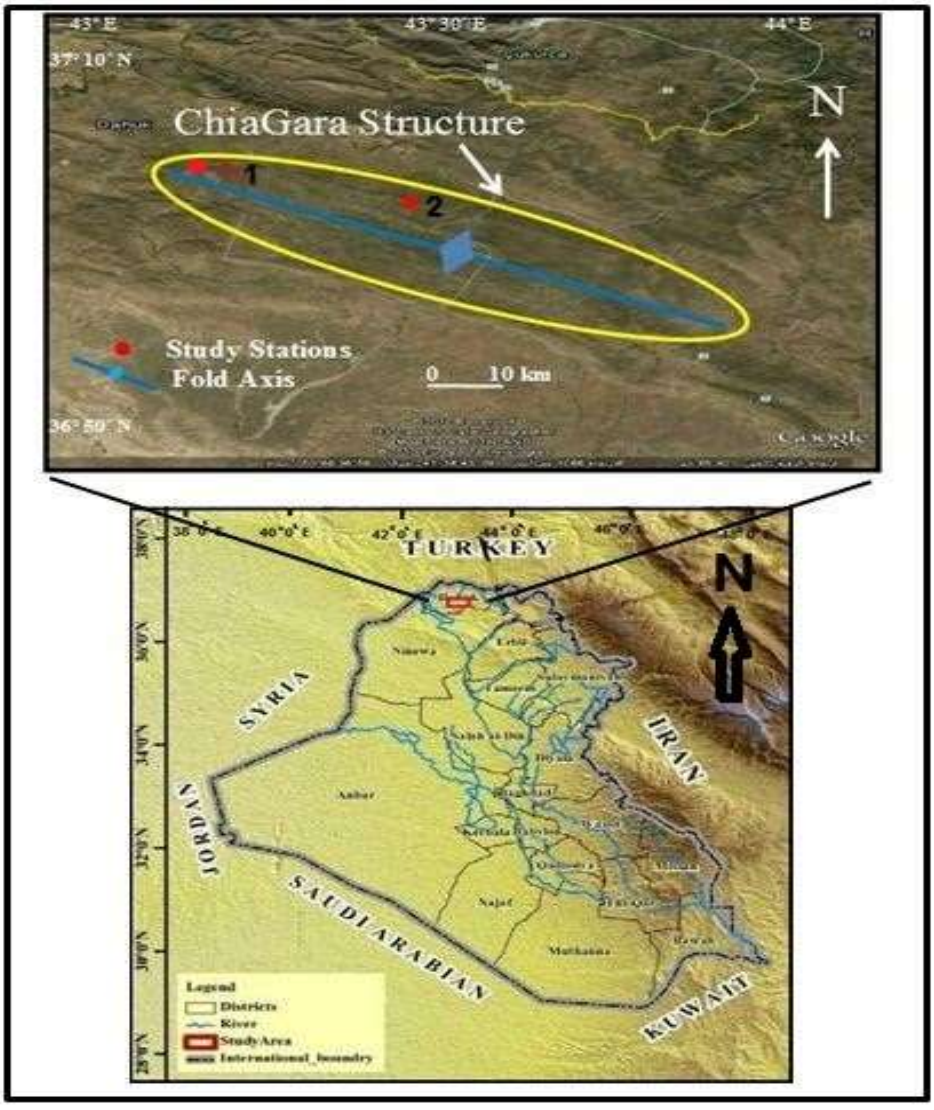

Figure 1- Satellite image showing the study area [9]

This study aims to determine the orientation and magnitudes of the paleostress, calculate the stress ratio (R) depending on Bott law, and understand the dynamics of the study area.

Geological Setting

Tectonically, the study area belongs to the unstable shelf represented by the High Folded Zone [10,11]. The exposed formations range in age from the Late Triassic (Kurra Chine Formation) to the Late Miocene (Injana Formation). A brief description of these formations from the oldest to the youngest is provided in the following section [12]:

Kurra Chine Formation: The age of the formation is Late Triassic. It consists of black limestone beds, thick dolomite beds and thin beds of shale. The thickness of the formation ranges between 118-834 m. **Baluti Formation:** The age of the formation is Early Jurassic. It consists of grey shale, oolitic limestone and dolomite beds. The thickness of the formation is 60-67 m. **Sarki Formation:** The age of the formation is Early- Middle Jurassic. It consists of dolomitc limestone beds, shale and marls. The thickness of the formation is 50-60 m. **Sehkaniyan Formation:** The age of the formation is Middle Jurassic. It comprises black bituminous dolomite beds and organic limestone. The thickness of the formation is 40-62 m. **Naokelekan Formation**: The age of the formation is Late Jurassic. It consists of bituminous limestone and thin bedded fossiliferous dolomitic limestone. The thickness of the formation is 20 m. **Barsarin Formation:** The age of the formation is Late Jurassic. It comprises limestone and dolomitic limestone. The Thickness of the formation is 20 m. **Chia Gara Formation:** The age of the formation is Late Jurassic. It comprises thinly bedded limestone, marly limestone beds, and shale. The thickness of the formation is 25 m. **Garagu Formation:** The age of the formation is Late Jurassic –Early Cretaceous. It consists of oolitic sandy limestone. The thickness of the formation is 20-92 m. **Sarmord Formation:** The age of the formation is Early Cretaceous. It comprises brown marls and beds of clayey limestone. The thickness of the formation is 20 m. **Qamchuqa Formation:** The age of the formation is Early Cretaceous. It consists of dark grey, hard and bedded to massive limestone and dolomite. The thickness of the formation is 250-362 m. **Akra- Bekhme Formation:** The age of the formation is Late Cretaceous. It consists of bituminous secondary dolomite and limestone. The thickness of the formation is 300-400 m. **Shiranish Formation**: The age of the formation is Late Cretaceous. It comprises thinly bedded marly limestone. Limestone of this formation is hard jointed and fractured. The thickness of the formation is 202 m. **kolosh Formation:** The age of the formation is Paleocene- Early Eocene. It consists of fine clastic, which are sandstone, siltstone and claystone. The thickness of the formation is 100-400 m. **Gercus Formation:** The age of the formation is Middle Eocene. It consists of red claystone and siltstone along with few sandstone and conglomerate. The thickness of the formation is 320-546 m. **Pila Spi Formation:** The age of the formation is Middle- Late Eocene. It comprises claystone and marls with alternation of thick limestone. The thickness of the formation is 318-565 m. **Fat'ha Formation:** The age of the formation is Middle Miocene. It consists of claystone and marls with alternation of thick limestone. The thickness of the formation is 219-497 m. **Injana Formation:** The age of the formation is Late Miocene. It comprises thin bedded sandstone, siltstone, marls, and reddish brown and brownish grey claystone. The thickness of the formation is 400-900 m.

Methodology

1: Faults Orientation Analysis Using Right Dihedral Method

Many authors [2,3,4,5,13,14] used the fault slip data to calculate orientations of the paleostress field.

Right dihedral method was used to determine an orientation of principal stresses axes (σ1, σ2 and σ3) of the study area. The maximum principal stress (σ1) and the intermediate principal stress (σ2) were horizontal, whereas the minimum principal stress (σ3) was sub vertical. The dips of these faults were to the north and south directions in both stations of the study area (Plates 1 and 2, Figures- 2 and 3). The determination of the principal stress axis orientations were performed as previously described [15].

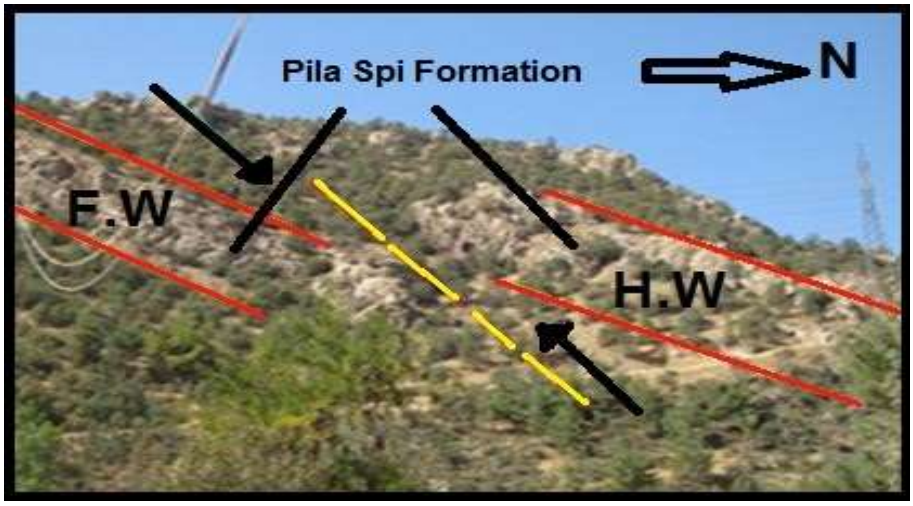

Plate 1- Thrust Fault in Pila Spi Formation in the north limb of Chia Gara Structure in the study area.

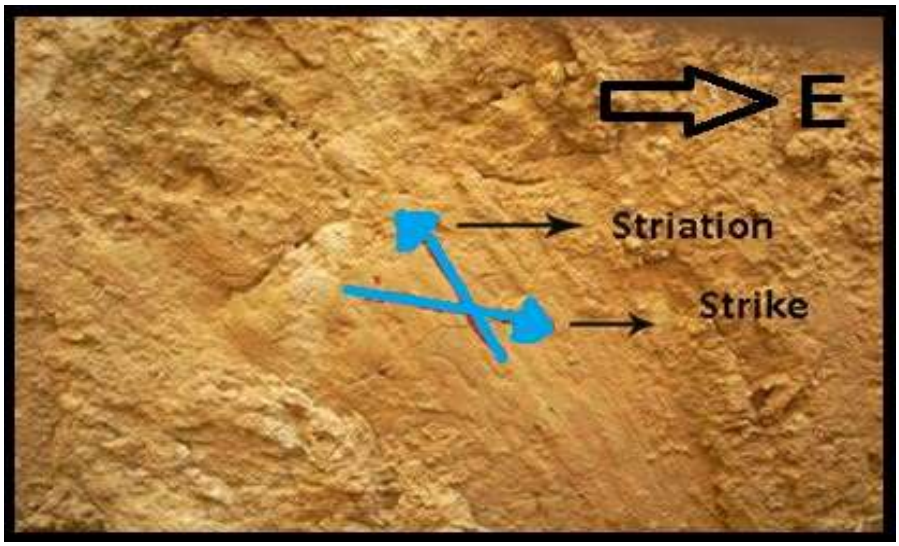

Plate 2- Striation on the fault plane in the hinge area of Chia Gara Structure in the study area.

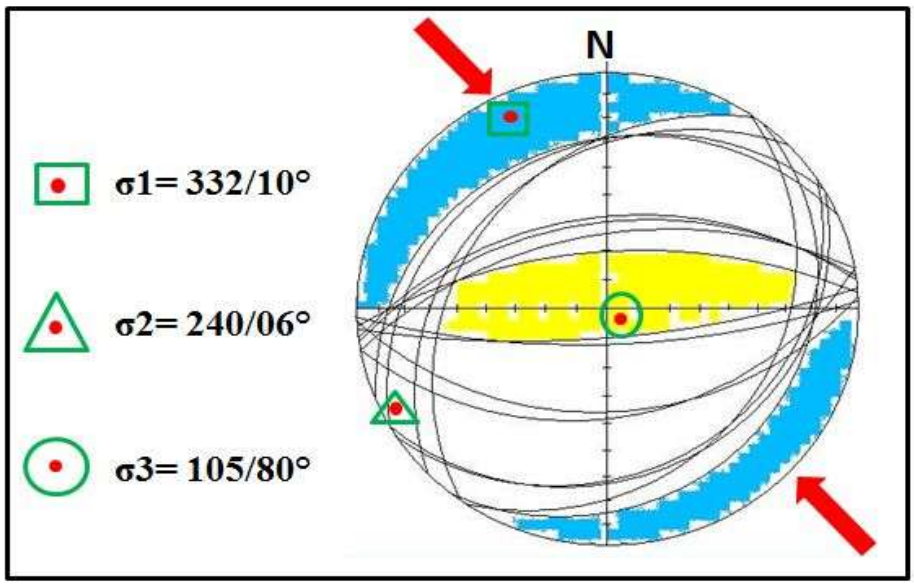

Figure 2- Right dihedral method showing the distribution orientation of the principal stress axes in station one of the study areas.

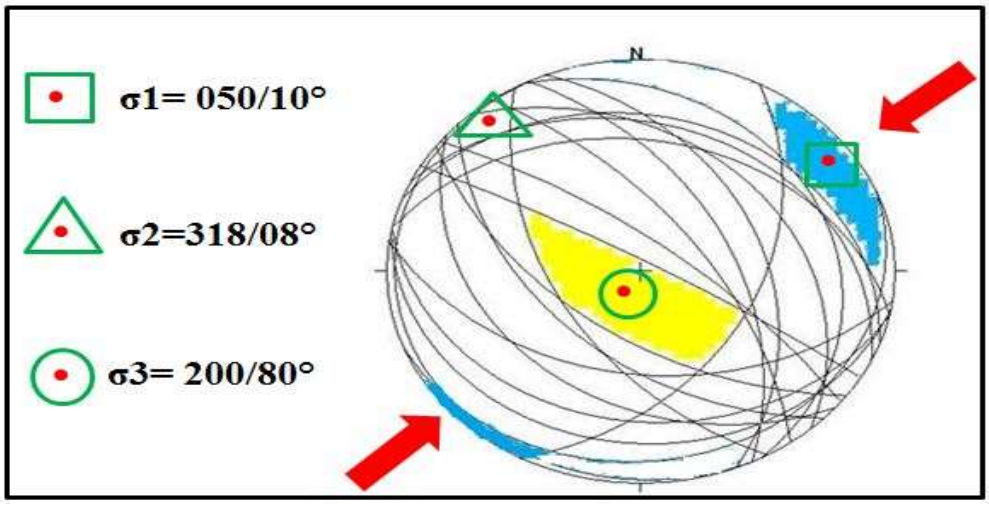

Figure 3- Right dihedral method showing the distribution orientation of the principal stress axes in station two of the study area.

2: Determination of the Paleostress Magnitudes Using Mohr Diagram

The value of the vertical stress (σv) can be determined by estimating the lithostatic load and one of the principal stress axes. At the time of the tectonic event, the depth can be determined as well as the average density of the overlying rocks. Additional information on the value of one principal stress can be obtained using the following equation:

$\sigma v = \rho g z$ …… [16-18]

where ρ is the average density of the rocks (kg/m³), g is the acceleration of gravity (m/s²), and z is the depth (m).

Lisle graph and Mohr diagram were used to represent the state of stress (Figure – 4). Mohr Plotter Software was used to determine paleostress magnitudes. The angles (α, β, γ) were measured between the pole to the slip plane (N) and the orientation of the principal stress axes (σ1, σ2 and σ3, respectively) of each fault. To determine the stress ration (R) value of all faults, Bott law was applied [19].

$R = \tan\theta\, Im - I^2 n / n\text{-}n^3$ ……..……... [19].

where R is the ratio of the principal stress, θ is the pitch angle, and I, m, and n are the cosine values of the angles α, β, and γ, respectively, as shown in Tables -1 and 2.

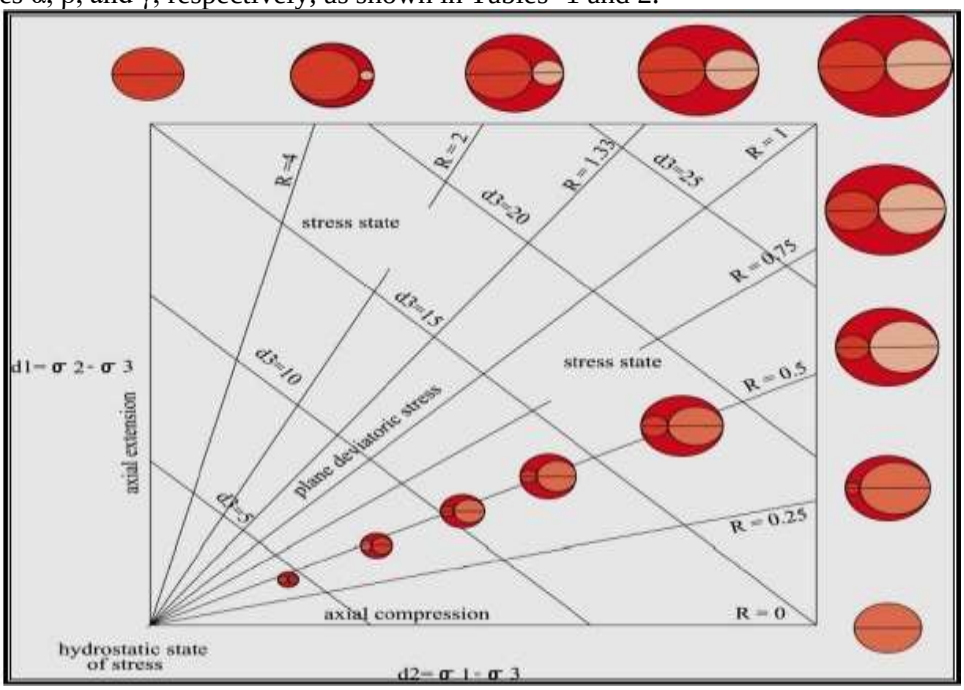

Figure 4- Lisle graph of the stress states representation [20].

Table 1- The magnitude of the stress ratios (R) for faults in station one of the study area.

NO.	Fault plane D.D/D.A	Pitch (ɵ)	tan (ɵ)	(α)	(β)	(ɣ)	R= tanɵIm – I² n / n-n³
1	356/70°	70° NW	2.74°	58°	59°	63°	1.7
2	350/64°	66° NW	2.24°	59°	62°	59°	1.1
3	352/60°	80° NW	5.67°	32°	84°	°64	2.5
4	353/58°	75° NW	3.73°	°33	83°	°64	1.4
5	178/58°	78° SE	4.70°	°55	°89	°36	0.3
6	175/60°	80° SE	5.67°	°69	°71	°41	0.6
7	179/52°	69° SE	2.60°	45°	°80	°55	0. 2
8	177/54°	72° SE	3.07°	°50	°70	°60	0. 2

Table 2- The magnitude of the stress ratios (R) for faults in station two of the study area.

NO.	Fault plane D.D/D.A	Pitch (ɵ)	tan (ɵ)	(α)	(β)	(ɣ)	R= tanɵIm - I² n / n-n³
1	054/70°	70° NW	2.74°	79°	82°	°19	0.36
2	240/62°	65° SE	2.14°	66°	58°	°56	0.92
3	224/58°	70° SE	2.74°	71°	60°	49°	0.84
4	064/60°	54° NW	1.37°	°87	71°	22°	0.12
5	012/38°	75° SE	3.73°	85°	62°	33°	0.48
6	048/40°	60° NW	1.73°	°82	84°	14°	0.01
7	068/50°	70° NW	2.74°	°80	87°	13°	0.16
8	216/65°	80° NW	5.67°	67°	85°	28°	0.2
9	038/78°	70° SE	2.74°	°79	79°	22°	0.41
10	030/86°	80° SE	5.67°	83°	82°	11°	1.7

Results

Several authors studied cohesion strength of the sedimentary rocks and they showed that the range of the cohesion strength values range between zero (0) bars, indicating no stick between the two blocks of faults, and 100 bars [1], [2], [3], [4], [5], [13], [14], [21], [22], [23] and [24]. Several authors used an internal friction angle (ϕ) for the rocks of 45° [1], [2], [3], [4], [5], [13] and [14]. Two friction sliding line angles of thrust faults were measured experimentally by the author for fault surfaces. These measurements showed that the average of the minimum friction sliding line angle is 25˚ for the smooth fault surfaces, as limestone rocks, while the average of the maximum friction sliding line angle is 35˚ for the rough fault surfaces, as sandstone rocks.

Thrust faults measurements were obtained from the hinge area to the north limb of Chia Gara Structure of the study area. The depth of the rocks was measured at the field and it was equal 5072 m. The acceleration of gravity (g) was equal to 9.8 m/ s², whereas the average density of the sedimentary rock was estimated to be 2300 kgm/m³. Therefore, the stress can be estimated as vertical ($\sigma v = \sigma 3$).

Mohr diagram was drawn depending on the stress ratio (R) magnitude (R=1 in station one and R=0.5 in station two), while the points (poles of the faults) were plotted depending on the angles (α, β, γ) on these circles. The plot points in Mohr diagram should be found above the sliding line and beneath the failure envelope. The result obtained by the application of this method is summarized in Figures- 5 and 6 and Table -3.

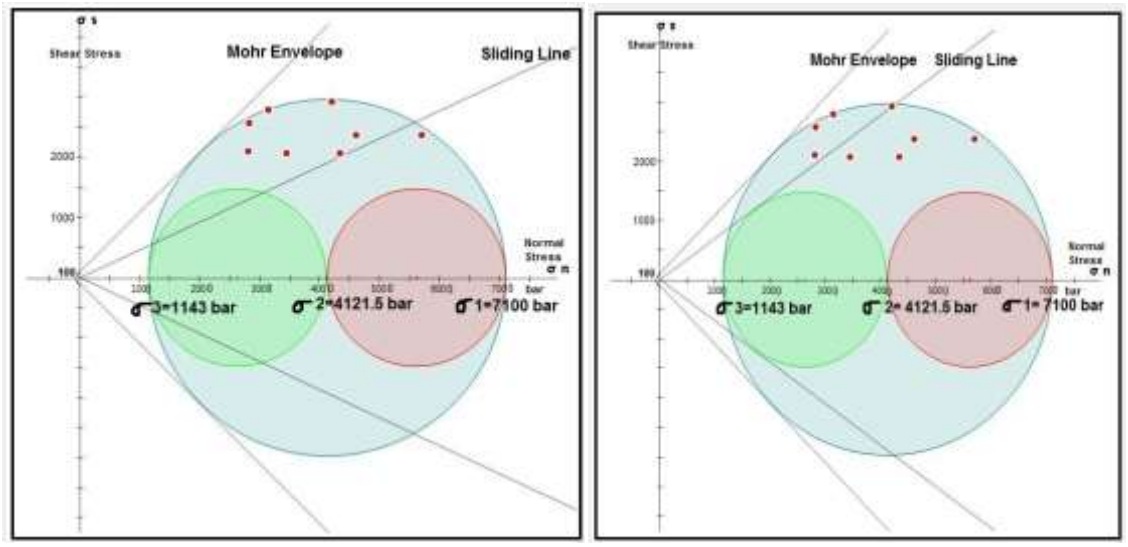

(a) (b)

Figure 5- Mohr diagram to calculate the magnitudes of the principal stresses in station one of the study area. (a) The friction sliding line 35°. (b) The friction sliding line 25°.

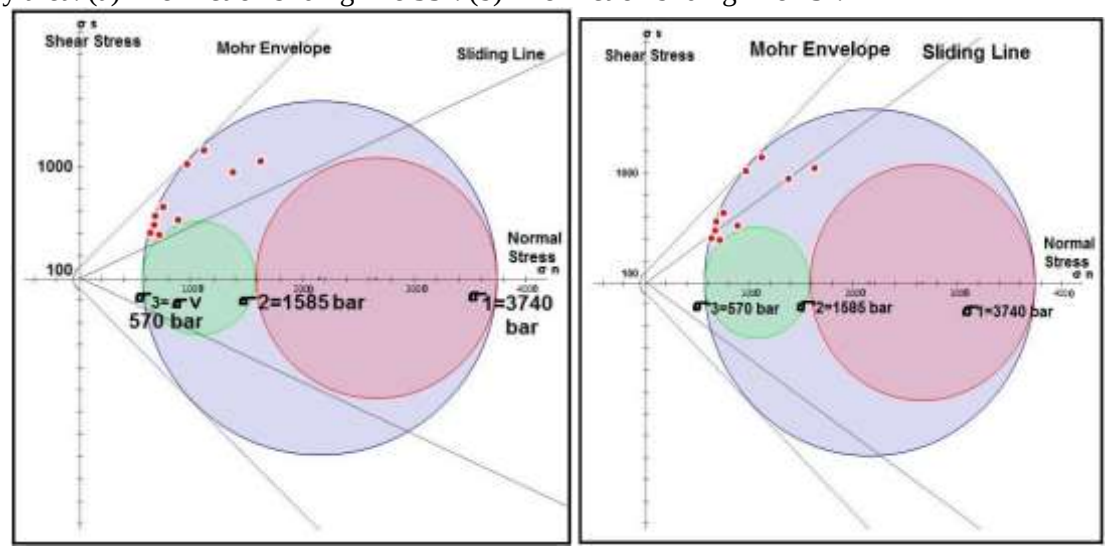

(a) (b)

Figure 6- Mohr diagram to calculate the magnitudes of the principal stresses in station two of the study area. (a) The friction sliding line 35°. (b) The friction sliding line 25°.

Table 3- The magnitudes of the principal stress (σ1, σ2 and σ3) of the study area.

No of Station	σ1 bar	σ2 bar	σ3=σ v bar	Depth (m).	Density Kg/m³	Hydrostatic Pressure bar = (σ 1+ σ 2+σ 3) /3	Cohesion Strength= (σ 1- σ 3) bar	d2 bar (σ 1- σ 2)	d1 bar = (σ 2- σ 3)
1	7100	4121.5	1143	5072	2300	4121.5	5957	2978.5	2978.5
2	3740	1585	570	2530	2300	1965	3170	2155	1015

Thrust faulting in Chia Gara structure involved a compression regime (σ1) which was almost horizontal, sub vertical extensional axes (σ3) , and an intermediate axis (σ2) which was horizontal (Figure -7).

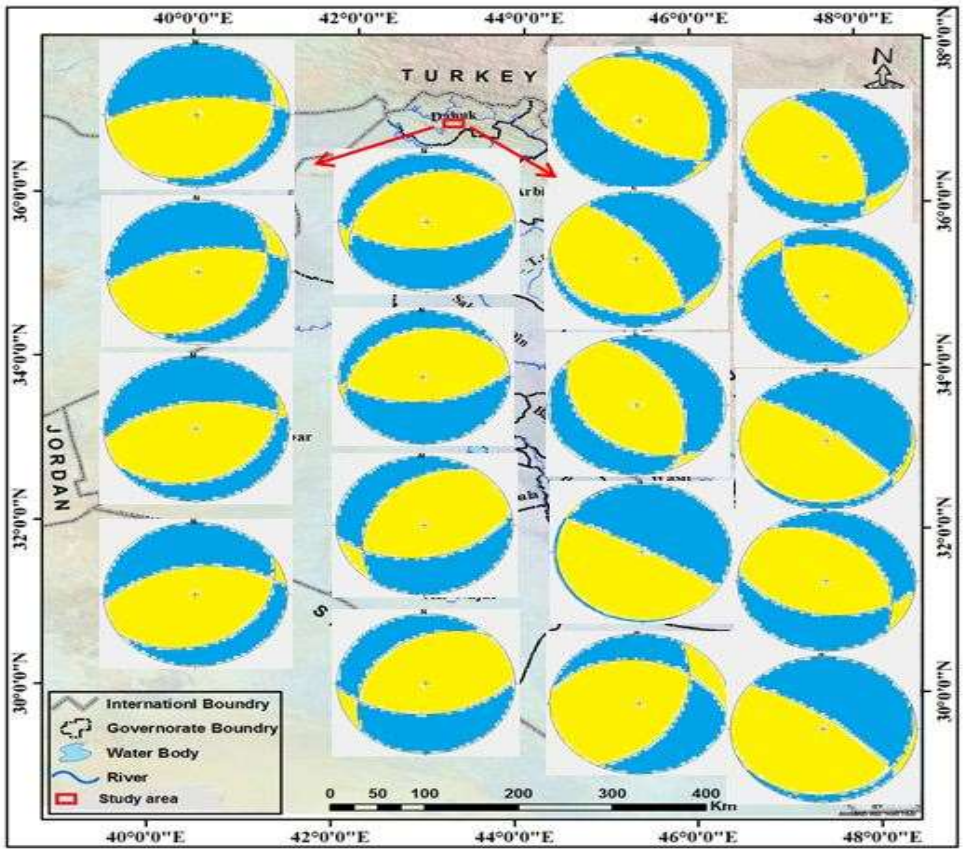

Figure 7- Faults solution in a lower hemisphere equal- area projection according to the present study.

The yellow color is an extensional field which contains (σ3) and the blue color is the contractional field which contains (σ1).

Discussion

The rocks of the Mesozoic -Cenozoic Eras (Kurra Chine Formation–Injana Formation) were studied to determine the magnitudes and orientations of the paleostresses based on field data, Right dihedral method, Mohr diagram, Bott Law and Lisle graph. Mohr diagram showed that the poles of the thrust faults lie between the sliding lines and the failure envelope. Mohr diagram reflects the relationship between the shear stress and the effective normal on the fault planes, with a proportional relationship between the reactivation on the faults and shear stress. The resulted diagram showed high magnitudes of normal stresses. The study results showed that the orientations of stress axes and their magnitudes are sufficient for the reactivated faults. Magnitudes of the stress were not constant and the stress ellipsoid was different. This difference may refer to the difference of the stress fields, the depth variation, and the stress magnitudes which have changed over the time. The high magnitudes of the normal stresses may refer to the active tectonic event which led to the deformation of the area during the Mesozoic Era and the Tertiary period.

Conclusions

The study area was affected by a compression stress regime during the Alpine Orogeny compression. Mohr diagrams showed two sets of poles of the thrust faults; the first set is reactivated faults, which lie between the sliding line and the failure envelope, while the second set is inactive faults with poles distributed along the boundaries of Mohr Circles. Generally, the poles of faults indicate low shear stress and high normal stress, indicating no slip under these conditions. The shear stress was sufficient to produce the slip along the fault surfaces, otherwise it cannot be attributed to another mechanism. If the σ1 is not perpendicular to the fault surface and the value of σ3 is higher than the frictional slide, then the slip will happen. The value of shear stress for the slip will increase with increasing the normal stress, as indicated from the correlation between Figures- 5 and 6. Distribution of the stress ratio magnitudes on Lisle graph showed stress ratio mean values (R=1 in station one and R= 0.5 in station two) which indicated that the states of the stress were plane

deviatoric and flattening, respectively, or, in other words, an axial compression of stress ($\sigma 1 > \sigma 2 > \sigma 3$).

References

1. Al- Obaidi, M. R. **1978.** A Study of Geological Structures of Jabel Sinjar, M.S. Thesis, University of Baghdad, Baghdad, Iraq, 238p.
2. Al-Obaidi, M. R. **1994.** Stress field determination (Orientation and Magnitudes) and their relation to structural trends and overburden thickness for Sinjar and Bashiqa structures, North of Iraq , *Journal of Science . Iraq*, **35**(2): 365- 380.
3. Handula, R. E. **1997.** *Structural and stress analysis in the folded area north and northeast of Iraq*, M.S. Thesis, University of Baghdad, Baghdad, Iraq, 126p.
4. Al- Diabat, A. A., Al-Obaidi, M. R. and Atalla M. **2003.** Magnitudes of the Paleostresses at the Eastern Rim of the Dead Sea Transform Fault, *Journal of Pure Sciences*, **30**(1): 1-13.
5. Al- Hachem, A. E. **2018.** The Structural and Tectonic Analysis of Missan area Southeastern part of Iraq, Ph. D. Thesis. University of Baghdad, Baghdad, Iraq, 205p.
6. Abdulhassan , A. K. **2019.** Paleostress Analysis of Selected Structures in Southeastern Part of Low Folded Zone/ IRAQ, Ph. D. Thesis. University of Baghdad, Baghdad, Iraq, 211p.
7. Kaymaki, N. **2006.** Kinematic development and paleostress analysis of the Denizli Basin western Turkey, *Journal of Asia Earth Sciences*, **27**: 207-222.
8. Al-Jumaily, I . S., Adeed, H . G., Al- Hamdani , R. K. and Dawlat, M. S., **2012.** Structural Analysis and Tectonic Interpretation of Brittle Failure Structures at Perat Anticline-NE Iraq. *Iraqi National Journal of Earth Science*, **12** (2): 17-42.
9. http:// www. Google earth image, **2019**.
10. Al- Khadimi, J. A., Sissakian, V. K., Fattah , A. S. and Deikaran, D. B. **1996**. *Tectonic map of Iraq*, (Scale: 1:1 000000) S. E. of Geological Survey and Mining, Iraq.
11. Numan, N.M. **1997.** A plate tectonic scenario for the Phanerozoi succession in Iraq**,** *Jour. Geol. Soc. Iraq*, **30**(2): 85-110.
12. Jassim, S. Z. and Goff, J. C. **2006**. *Geology of Iraq***.** Published by Dolin, Prague Moravian Museum, Brno, Czech Republic, 341p.
13. Abdualhassan, A. K. and Al-Obaidi, M. R. **2018.** Determination of the Paleostress Magnitudes of the Eastern Part of the Low Folded Zone, E- Iraq, *Indian Journal of Natural Sciences*, **9**(50): 15145-15152.
14. Al-Hachem, A. E. and Al – Obaidi, M. R. **2018**. Determination of the Paleostress Orientations and Magnitudes for Missan Structures, Southeastern Iraq**.** *Journal of University of Babylon for Pure and Applied Sciences*, **26**(10): 213-223.
15. GEOrient ver. 9.5, 2011**.**
16. Suppe, J. **1985**. *Principle of structural geology*. Prentile- Hall, Inc. Engle wood cliffs, New Jersey.
17. Sassi, W. and Carey – Gailhardis, E. **1987**. Interpretation mechanique du glissementsur les failles: Introduction dun critere de frottement **"**, *Annales Tectonicae*, **1**: 139- 154.
18. Fossen, H. **2012**. *Structural Geology:* United States of America, Cambridge University Press, third edition, 463p.
19. Bott, M. H. **1959**. The mechanics of oblique slip faulting, *Geol. Mag.*, **96**: 109-117.
20. Lisle, J. **1979**. The representation and calculation of the deviatoric component of the Geological stress tenser**.** *Journal of Structural Geology*, **1**: 317-321.
21. Al- Obaidi, M. R. and Al-Kotbah, A. M. **2003**. The magnitudes of the paleostresses of Yemen Faults in the sedimentary cover. *Faculty of Science Bulletin*, **16**: 95-109.
22. Al- Banna, A. S. and Ali, K.K. **2018**. The Transform Tectonic Zone between Two Parts of the Platform in Iraq: a Review Study. *Iraqi Journal of Science*, **59**(2C): 1086-1092.
23. Al- Banna, A.S. and Al-Kishef, D.s. **2019**. Evalution of the Tectonic Boundaries in Tikrit- Kirkuk Area Using Potential Data, North- Central Iraq. *Iraqi Journal of Science*, **60** (3): 528-535.
24. Al Banna, A.S. and Al-Namar, A.F. **2019**. Gravity and Magnetic Interpretation of Study Deep Crustal Structures in Karbala and Surrounding Areas- Central Iraq. *Iraqi journal of Science*, **69**(3): 536-544.